Available online at www.sciencedirect.com

ScienceDirect

Energy Procedia 92 (2016) 29 – 36

Energy Procedia

6th International Conference on Silicon Photovoltaics, SiliconPV 2016

Lifetime analysis for defect characterization in kerfless epitaxial silicon from the porous silicon process

Catherin Gemmel[a]*, Jan Hensen[a], Sarah Kajari-Schröder[a], Rolf Brendel[ab]

[a]*Institute for Solar Energy Research (ISFH), Am Ohrberg 1, 31860 Emmerthal, Germany*
[b]*Institute for Solid State Physics, Leibniz Universität Hannover, Appelstrasse 2, D-30167 Hannover, Germany*

Abstract

Kerfless epitaxial silicon from the porous silicon (PSI) process is a promising alternative for standard wafers. They allow the reduction of PV costs by combining high material quality at reduced production costs. We evaluate the minority carrier lifetime of p-type and n-type epitaxial silicon layers fabricated with the PSI process by means of photoconductance decay measurements. For p-type layers we observe a strong injection dependence of the lifetime that we attribute to bulk Shockley-Read-Hall (SRH) recombination. We determine two limiting defects K3.6 and K157 that describe the injection dependence of 9 samples grown in one batch. Defect K3.6 has a symmetry factor of k=3.6 and is similarly concentrated in all 9 investigated samples. Its concentration decreases upon high temperature processing with and without phosphorous diffusion. The defect K157 has a symmetry factor of k=157 and a higher concentration in samples with a higher porosity in the starting layer. As a consequence of the k-factors being larger than unity the identified defects are less detrimental in n-type silicon than p-type silicon. Accordingly, we fabricate n-type epitaxial layers for which we measure effective lifetimes up to 1330±130 µs at $\Delta p = 10^{15}$ cm $^{-3}$.

Peer review by the scientific conference committee of SiliconPV 2016 under responsibility of PSE AG.

Keywords: kerfless; mono-epitaxy, silicon; lifetime; Shockley-Read-Hall, symmetry factor

1. Introduction

Kerfless crystalline silicon produced by epitaxy on porous silicon (PSI process) is a promising approach for reducing costs in silicon photovoltaics [1,2] while maintaining the material's minority carrier lifetime [3,4]. While

* Corresponding author. Tel.: +49 (0)5151-999-430; fax: +49 (0)5151-999-400.
E-mail address: gemmel@isfh.de

Peer review by the scientific conference committee of SiliconPV 2016 under responsibility of PSE AG.
doi:10.1016/j.egypro.2016.07.006

the approach requires new manufacturing technologies it is also a promising paths to lower silicon usage [5]. High conversion efficiencies are a must in Si photovoltaics and thus a high quality of the silicon material, i.e. a high minority carrier lifetime, is essential. To ensure high minority carrier lifetimes it is necessary to avoid contaminants and structural defects in the epitaxial layer [3,6]. Metallic contaminants that are well known to influence lifetime negatively are e.g. iron, chromium or platinum. The latter was recently found to be the dominant lifetime limiting defect in epitaxial silicon from the PSI process introduced during the electrochemical etching [7]. For this reason ISFH avoids direct contact between the electrolyte and metallic electrodes since many years. Powell et al. reported a lifetime increase >500x during phosphorous diffusion by reducing the platinum concentration in the epitaxial layer. Studies show that also the amount of other metallic contaminants can be reduced by applying appropriate post-wafering processes e.g. gettering [3,8].

The identification of lifetime limiting defects and their origin is essential for improving the epitaxial layer quality [3]. The highest reported effective lifetimes in p-type epitaxial kerfless layer is 342±34 µs for a 1.79 Ωcm material and a wafer thickness of 95 µm sample after gettering [3]. A larger lifetime of 780 µs was measured for a 180 µm thick 2 Ωcm p-type epitaxial wafer [8]; no information on post-wafering processes are given here. For n-type layers the highest reported lifetimes are >2 ms [8].

Here, we investigate the bulk SRH lifetime of epitaxial silicon layers extracted from injection dependent measurements. We apply SRH lifetime analysis [9,10] to identify the lifetime limiting defects in our epitaxial kerfless p-type silicon. In analogy to Petermann et al. [11] we find a strong injection dependency of the measured effective lifetime. We aim at relating injection dependent lifetime features to details of the processing sequence in order to find pathways for increasing the minority carrier lifetime. High temperature processing is one option for improving the lifetime, changing the conductivity from p- to n-type is another option.

2. Experiemental

We prepare samples in three steps: first anodic etching, second high temperature processing and last the lift-off and processing of the detached epitaxial layer.

We use anodic etching of 6” 14 Ωcm p-type polished CZ silicon wafers in order to form a porous double layer structure [2]. We etch a starting layer and then increase the current density to values of 100 to 160 mA/cm² to form a 220 nm thick highly porous layer. We use two etching setups with electrolytes that have slightly different HF concentrations. These two HF concentrations and the chosen current densities result in slightly different porosities and thickness values of the starting layer. Samples from one setup have a 1019±20 nm-thick starting layer with a porosity of 26±1 %; the samples from the other setup have a starting layer with 1184±60 nm thickness and a porosity of 20±1 %. We group the samples by the porosity of the starting layer into a set of HP samples with high porosity in the starting layer and a set of LP for samples with a lower porosity. In this work we investigate 6 samples from group HP (HP-1…-6) and 3 samples from group LP (LP-1…-3).

After etching, the wafers reorganize at a temperature of 1100 °C in hydrogen atmosphere. The highly porous layer transforms to the separation layer covered by a closed silicon film. Without vacuum break an 113±3 µm-thick p-type epitaxial layer grows (resistivity of 0.5±0.1 Ωcm) or an 112±3 µm-thick n-type (resistivity of 5.1±1 Ωcm) sample.

We define the lift-off area of 9x9 cm² at the central wafer position by laser-cutting the epitaxial layer. We mechanically lift off the defined area and remove the residual porous silicon in a KOH etching bath witch a concentration of 20 % and a temperature of 45 °C. Then we clean the samples with standard RCA and passivate both sides with 10 nm Al_2O_3 using plasma assisted atomic layer deposition (ALD). Finally, we anneal the samples at 425 °C for 15 min.

We measure the injection dependent lifetime with quasi steady state photoconductance (QSSPC) and infrared steady state photoconductance (IRSSPC) to cover a wide injection range. On the two samples HP-1 and LP-1 we measure injection dependent lifetimes at three positions (HP-1.1, -1.2, -1.3 and LP-1.1, 1.2, 1.3) in order to examine spatial homogeneity of the injection dependence. Additionally, we also use infrared lifetime imaging (ILM) at 70 °C with an illumination of 0.31 suns to measure the homogeneity of the lifetime distribution.

Furthermore, we apply two kinds of post-wafering high temperature processes. We laser-cut one sample from each group (HP-6 and LP-3) in three parts. We remove the passivation layer of two 4.5x4.5 cm² pieces of each sample and clean them with standard RCA; the remaining 3.5x9 cm² pieces stay in their original condition. Subsequently, we apply the two high temperature treatments with and without phosphorous diffusion on one 4.5x4.5 cm² piece of each sample. We refer to these processes as gettering and annealing, respectively. The gettering starts with a 42±1 Ω/□ phosphorous diffusion. After cool down from the diffusion temperate the temperature is held at 600 °C for 1 hour. The annealing process has the same thermal profile as the gettering process but no phosphorous glass is applied. We then etch 1.5±0.5 µm from the surface regions of the four temperature treated samples using KOH and subsequently clean and passivate the samples. Finally, we repeat the lifetime measurements with QSSPC, IRSSPC. Additionally we getter sample HP-5 in the same way and measure it with ILM before and after the treatment.

Using the measured effective lifetime τ_{Ref} of W_{Ref} = 300 µm thick p-type FZ reference sample with the resistivity of 2±0.2 Ωcm we determine the injection dependent effective surface recombination velocity S_{eff} (SRV) for p-type epitaxial layers by applying

$$S_{eff} = \frac{W_{Ref}}{2 \times \tau_{Ref} \times corr} \tag{1}$$

We assume that the effective lifetime of the reference samples measured by means of QSSPC is dominated by surface recombination and other recombination paths as e.g. SRH bulk recombination are negligible. We use a correction factor of corr=0.3 to take into account the higher doping concentration in the epitaxial layers compared to the reference sample [12]. We use the same approach for n-type samples using a 160 µm thick reference sample with the resistivity of 5.06 Ωcm without applying a correction factor.

We correct the measured effective lifetimes τ_{eff} for the lifetime limited by surface recombination τ_{Surf} and for intrinsic recombination consisting of Auger recombination τ_{Auger} and radiative recombination τ_{rad} using the models of Richter et al. [13] and Trupke et al. [14] to estimate the SRH-limited bulk lifetime τ_{SRH} of the epitaxial p-type samples using:

$$\frac{1}{\tau_{SRH}} = \frac{1}{\tau_{eff}} - \frac{1}{\tau_{Surf}} - \frac{1}{\tau_{Auger}} - \frac{1}{\tau_{Rad}} \qquad \text{with} \qquad \tau_{Surf} = \frac{W}{2 \times S_{eff}} \tag{2}$$

We analyze the calculated SRH bulk lifetime by fitting the residual lifetime with defect parameters. We determine the symmetry factors and the electron capture time constants of two independent SRH defects. These time constants represent the defect concentrations of the defects in the bulk.

3. Results

FIG. 1a shows the injection-dependent lifetimes of one p-type epitaxial silicon layer from each of the two sample groups HP and LP before and after annealing. We find a strong injection dependence of the bulk SRH lifetime. The bulk SRH lifetimes of 9 samples all grown in the same batch show similar characteristics for $\Delta n > 10^{15}$ cm^{-3}. However, samples from the LP and HP group show different characteristics at low injection levels $\Delta n < 10^{15}$ cm^{-3}. Whereas group LP samples show a lifetime saturating at 30 to 56 µs for $\Delta n < 10^{14}$ cm^{-3} group HP samples do not show a lifetime saturation and have lifetimes decreasing down to 10 µs for $\Delta n < 10^{13}$ cm^{-3}. At $\Delta n = 10^{15}$ cm^{-3} we determine bulk SRH lifetimes of 63±7 µs for samples from the group HP and up to 98±9 µs for samples from the group LP.

High temperature processing improves the lifetime by 10 to 20 %. We measure effective lifetimes of up to 98±15 µs at $\Delta n = 10^{15}$ cm^{-3} after gettering, which corresponds to a bulk SRH lifetime of 116±20 µs. We observe that

annealing and gettering result in the same lifetime improvement (not shown in the graph). For samples of both groups, the general trend in injection dependence does not change upon high temperature treatments neither with nor without phosphorous diffusion.

FIG. 1b shows ILM measurements of one 9x9 cm² sample from group LP before and after gettering under an illumination of 0.31 suns. Before gettering the arithmetic mean lifetime is 55.8±18.0 µs over the whole sample. The large variation results from the upper left corner with much lower lifetimes as for the right hand side of the sample. After gettering the lifetime distribution over the sample is much more homogeneous with 99.6±7.6 µs.

It is in principal possible do determine the energetic level of defects within the band gap by means of temperature dependent lifetime measurements [9,10]. Therefore, we measure lifetimes at various temperatures between room temperature and 200 °C. We use the samples before annealing because we expect them to have a higher defect concentration. However, we are not able to determine the trap depth in the experimentally accessible temperature regime. Hence, we conclude that the dominant defects are too deep in the band gap to extract the energetic position with measurements at only 200°C.

Some metal contaminants are known to form precipitates with boron which have a different impact on the lifetime than isolated contaminants [15]. Dissociation and association caused by heating or lightening of the precipitates changes the injection dependent lifetime. We apply temperature and light induced dissociation in order to identify iron or chromium as contaminants [16]. Since we observe no change in injection dependent lifetime upon dissociation and association we exclude these contaminants as the main lifetime limiting defects.

Finally we compare the outcomes from the analysis of the p-type layers with lifetime measurements of n-type layers also fabricated by the PSI process. For this we measure the injection dependent lifetime of similarly prepared n-type epitaxial layers by means of QSSPC. First investigated samples show effective lifetimes up to 1330±130 µs at $\Delta p=10^{15}$ cm^{-3} even before any high temperature processing.

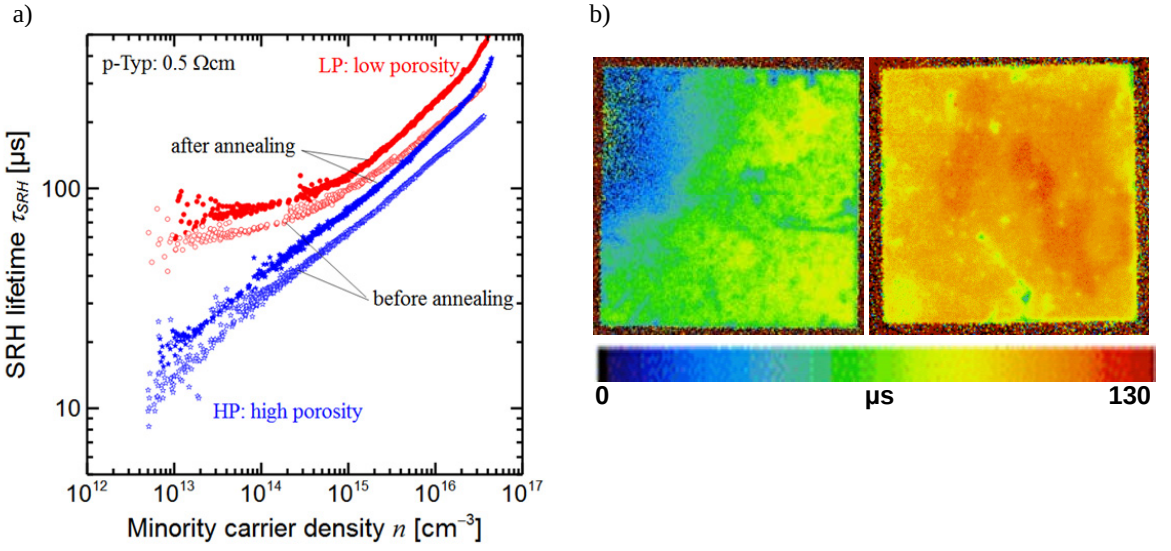

Fig. 1: a) Calculated bulk SRH lifetimes for one sample of each group LP and HP before and after annealing b) ILM measurement of a 9x9 cm² sample of group LP before (left) and after (right) gettering under an illumination of 0.31 suns at 70 °C

4. Discussion

Following the SRH equation [17] we calculate the injection dependence of the SRH bulk lifetime in order to fit the determined lifetime curves with:

$$\frac{1}{\tau_{SRH}} = \tau_{n0}\left(k\frac{n_0 + n_1(E_t) + \Delta n}{n_0 + p_0 + \Delta n} + \frac{p_0 + p_1(E_t) + \Delta n}{n_0 + p_0 + \Delta n} \right) \text{ with } \tau_{n0} = \frac{1}{N_T \sigma_n v_t} \quad (3)$$

where n_0 and p_0 are the thermal equilibrium concentrations of electrons and holes, respectively and n_1 and p_1 are the SRH densities as a function of the defect energy E_t. The symmetry factor $k=\tau_{p0}/\tau_{n0}$ is the ratio of the capture cross sections for electrons σ_n and holes σ_p, τ_{n0} is the capture time constant for electrons with the defect concentration N_t and v_t the thermal velocity.

Since the SRH lifetime is not sensitive to the defect energy over a wide range excluding the band gap edges [7] which we excluded by our temperature dependent measurements, we assume the defects to be at the mid-gap level. We fit the bulk SRH lifetimes of 9 samples from one batch with only two independent SRH defects [18]. The two defects are allowed to have different concentrations. Furthermore, we do not allow electron transitions from one defect level to the other. In the fitting procedure, the capture time constants $\tau_{n0,i}$ are the parameters that differ for all samples accounting for the defect concentration.

We determine two symmetry factors k_1=3.6 (+0.6/-0.7) and k_2=157 (+48/-25) that fit the lifetimes of all samples. We refer to these defects hereafter as K3.6 and K157, respectively. For the injection dependent lifetime measurements we expect an uncertainty of 10 %. Hence, we determine the uncertainty of the symmetry factors as fit parameter by systematically changing the effective lifetime by 10 %. While the symmetry factors have a relatively large uncertainty, the capture time constant is less sensitive to systematic variation of the measured lifetime. For $\tau_{n0,k=157}$ the uncertainty depends on the sample group: for HP we determine an error of (+2 %/ -9 %). For LP samples the error is higher; we determine (+12 %/ -18 %). For $\tau_{n0,k=3.6}$ we determine an uncertainty of ±4 %. This means that the capture time constants for K3.6 can be fitted more precisely than the capture time constants for K157.

FIG. 2 shows two exemplary fits of both groups HP and LP. K157 dominates at low injection whereas K3 shapes the lifetime curve at high injection. The coefficient of determination R^2 in the fitted range is 96.6±2.2 %. This means that the deviation of the simulation and the measured SRH lifetime is for 94 % of the points less than 10 µs. At very low injection (n<10^{14} cm^{-3}) the fit does not follow the lifetime of the HP samples. They show a decrease in lifetime to values as low as 10 µs and do not show any saturation. This behaviour cannot be explained by single SRH defect states, but for example by extended defects or defect clusters such as precipitates or dislocations [17].

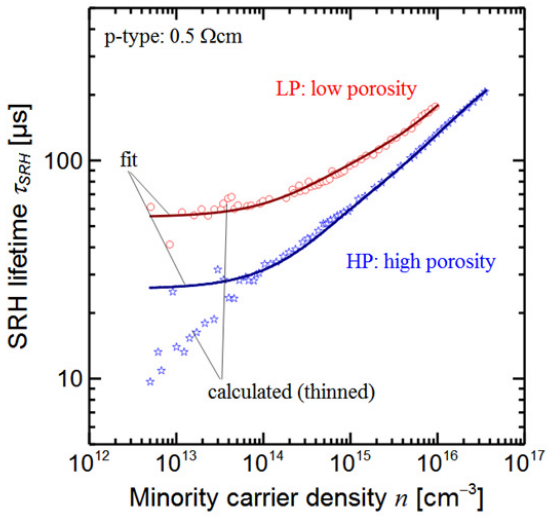

Fig. 2: Calculated bulk SRH lifetimes in dependence of the minority carrier density for one sample of each set of LP and HP samples before annealing with fitted curves

The fit results are depicted in FIG. 3. It shows the capture time constant rates, which are the inverse of the fitting parameters, for the two defects K3.6 and K157 for all samples. Defect K157 has a roughly three times smaller capture time constant rate (shaded green bars) in group LP compared to group HP, which in turn means a three times smaller concentration of the defect. Defect K157 does not show a significant change upon high temperature processing while defect K3.6 does. The capture time constant rate of K3.6 decreases, meaning that the defect concentration decreases upon gettering and annealing by about 30 % (see HP-6 and LP-3, blue bars).

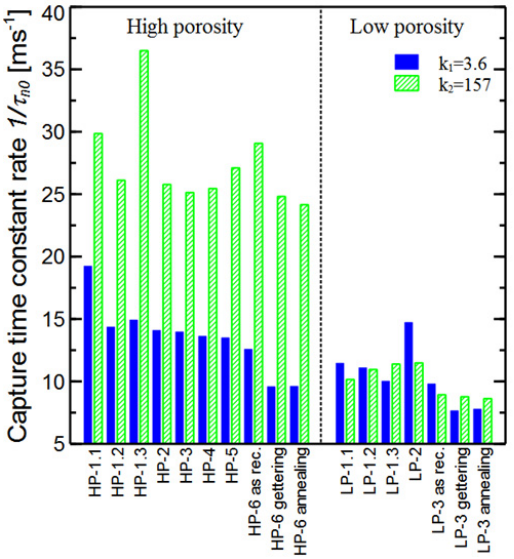

Fig. 3: Capture time constant rates determined by fitting two defects in the band gap center with k_1=3.6 and k_2=157 for two set of samples; HP-1.1 and LP-1.1 measured at three positions, HP-6 and LP- measured before and after temperature treatment

One difference between the groups HP and LP is the different porosity of the starting layer. We therefore speculate that K110 origins from structural defects that originate from epitaxial growth on an incomplete reorganization and less than ideal surface. It is known that contaminants tend to decorate dislocation sites [7]. A surface gettering would require the dissolution and the subsequent diffusion of the contaminants from these energetically preferable structural defects to the surface.

The two identified defects both have symmetry factors larger than one. This implies that their capture cross section for electrons is larger than that for holes. Consequently, these defects are more detrimental in p-type material than in n-type material. We thus expect a lower impact of these defects and hence less injection dependence in n-type material. Furthermore, due to the largly assymetric behaviour of K157 its impact in n-type silicon is expected to be even less than that of K3.6.

Assuming concentrations of K3.6 and K157 as in sample LP-3 after annealing, we calculate for n-type layers a bulk SRH lifetime of 466 µs at Δp=10^{15} cm^{-3} corresponding to an effective lifetime of 370 µs at Δp=10^{15} cm^{-3}. The calculated injection dependent effective lifetime is shown in FIG 4 as black stars. The figure also shows QSSPC measurements of our n-type kerfless epitaxial layers at two positions. We measure 482±48 µs at Δp=10^{15} cm^{-3}. Best area measurements reveal an effective lifetime of 1330±130 µs at Δp=10^{15} cm^{-3}. When fitting the lifetime measurement in an average area (green diamonds) we find a capture time constant of $\tau_{n0,1}$=175±10 µs corresponding to 34 % smaller defect concentration than in one of the best p-type samples after high temperature treatment. When speculating that the n-type samples respond to the high temperature treatment similar than the p-type samples we expect a lifetime improvement by 30 % from annealing or gettering. However, when fitting the best area QSSPC measurements, we find capture time constants of $\tau_{n0,1}$=12 ms and $\tau_{n0,1}$=16 µs. This means that in these regions defect

K157 is much more dominant than defect K3.6. For the latter we find on one hand the concentration to be 70 times smaller than in average region. On the other hand the concentration of K157 is 7 times higher.

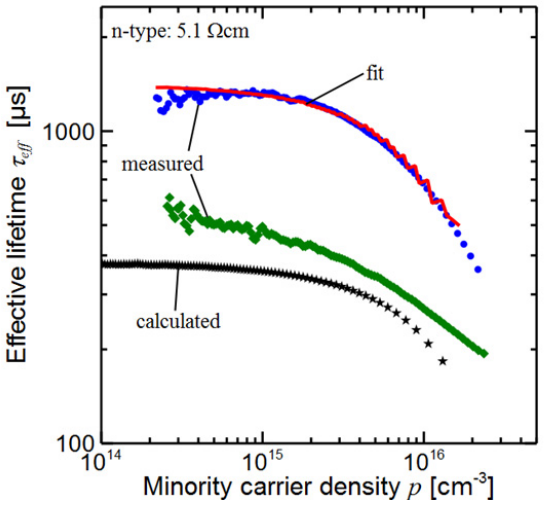

Fig. 4: Measured effective lifetime of n-type epitaxial layer at two spots (green diamonds, blue dots), calculated with K3.6 and K157 and concentrations as in LP-3 after annealing (black stars) and fitted with K3.6 and K157 and variable time constants (red line)

5. Conclusion

Lifetime measurements in p-type epitaxial silicon exhibit a strong injection dependence which can be fitted by SRH bulk recombination applying two independent defects with symmetry factors of k_1=3.6 (+0.6/-0.7) and k_2=157 (+48/-25). We observe different defect concentrations of K157 in two sample groups which are etched in two setups and with different porosities in the starting layer. Furthermore, we observe that K3.6 can be reduced by high temperature processes. We speculate that the different concentrations of K157 in the sample groups originate from the different characteristics of the porous starting layer and the resulting surface after reorganization. We hypothesize that a lower porosity in the starting layer leads to a more ideally closed surface and consequently to less structural defects in the epitaxial layer. This phenomenon is well described in literature [6,19]. While K157 cannot be reduced by high temperature treatments, K3.6 does. However, since gettering and annealing leads to the same lifetime improvement we expect that gettering is not driven by the phosphorous diffused layer. We speculate that the gettering either takes place at the surface or that the defect becomes inactive in a different way.

We measure effective lifetimes of up to 98±15 µs at $\Delta n=10^{15}$ cm^{-3} after gettering in p-type samples, which corresponds to a bulk SRH lifetime of 116±20 µs. As a consequence of the k-factors being larger than unity the identified defects are less detrimental in n-type silicon than p-type silicon. For similarly fabricated n-type samples we measure in best areas an effective lifetime of 1330±130 µs at $\Delta p=10^{15}$ cm^{-3}. We expect to be able to improve this lifetime by high temperature processing because of the positive effects observed upon high temperature processes for K3.6 in p-type material.

References

[1] Rolf Brendel. A novel process for ultrathin monocrystalline silicon solar cells on glass. In: 14th European Photovoltaic Solar Energy Confrence; 1997, p. 1354–8.
[2] Tayanaka H, Matsushita T (ed). Separation of thin epitaxial films on porous Si for solar cells; 6th Sony research forum; Tokyo, 1996.
[3] Powell DM, Hofstetter J, Fenning DP, Hao R, Ravi TS, Buonassisi T. Effective lifetimes exceeding 300 µs in gettered p-type epitaxial kerfless silicon for photovoltaics. Appl. Phys. Lett. 2013;103:263902, doi:10.1063/1.4844915.

[4] Radhakrishnan HS, Martini R, Depauw V, van Nieuwenhuysen K, Debucquoy M, Govaerts J, Gordon I, Mertens R, Poortmans J. Improving the Quality of Epitaxial Foils Produced Using a Porous Silicon-based Layer Transfer Process for High-Efficiency Thin-Film Crystalline Silicon Solar Cells. IEEE J. Photovoltaics 2014;4:70–7, doi:10.1109/JPHOTOV.2013.2282740.
[5] D. M. Powell, M. T. Winkler, A. Goodrich, T. Buonassisi. Modeling the Cost and Minimum Sustainable Price of Crystalline Silicon Photovoltaic Manufacturing in the United States. IEEE Journal of Photovoltaics 2013;3:662–8, doi:10.1109/JPHOTOV.2012.2230056.
[6] Milenkovic N, Drießen M, Weiss C, Janz S. Porous silicon reorganization: Influence on the structure, surface roughness and strain. Journal of Crystal Growth 2015, doi:10.1016/j.jcrysgro.2015.09.025.
[7] Powell DM, Markevich, V. P., Hofstetter J, Jensen, M. A., Morishige, A. E., Castellanos S, Lai B, Peaker, A. R., Buonassisi T. Exceptional Gettering Response on Epitaxial Grown Kerfless Silicon. Journal of Applied Physics;submitted.
[8] Hao R, Ravi TS, Siva V, Vatus J, Miller D, Custodio J, Moyers K, Chen C, Upadhyaya A, Rohatgi A. High efficiency solar cells on direct kerfless 156 mm mono crystalline Si wafers by high throughput epitaxial growth. In: 2014 IEEE 40th Photovoltaic Specialists Conference (PVSC), p. 2978–82.
[9] Schmidt J. Temperature- and injection-dependent lifetime spectroscopy for the characterization of defect centers in semiconductors. Appl. Phys. Lett. 2003;82:2178, doi:10.1063/1.1563830.
[10] Rein S, Lichtner P, Glunz SW. Advanced lifetime spectroscopy: unambiguous determination of the electronic properties of the metastable defect in boron-doped - Photovoltaic Energy Conversion, 2003. Proceedings of 3rd World Conference on. In: IEEE PV Specialists Conference, editor. Proceedings of the 3rd World Conference on Photovoltaic Energy Conversion: Joint conference of 13th PV Science & Engineering Conference, 30th IEEE PV Specialists Conference, 18th European PV Solar Energy Conference; Osaka International Congress Center \"Grand Cube\", Osaka, Japan, 11 - 18 May 2003.
[11] Petermann JH, Ohrdes T, Altermatt PP, Eidelloth S, Brendel R. 19% Efficient Thin-Film Crystalline Silicon Solar Cells From Layer Transfer Using Porous Silicon: A Loss Analysis by Means of Three-Dimensional Simulations. IEEE Trans. Electron Devices 2012;59:909–17, doi:10.1109/TED.2012.2183001.
[12] Werner F. Atomic layer deposition of aluminum oxide on crystalline silicon: Fundamental interface properties and application to solar cells. Dissertation, Gottfried Wilhelm Leibniz Universit at Hannover. Hannover; 2013.
[13] Richter A, Werner F, Cuevas A, Schmidt J, Glunz SW. Improved Parameterization of Auger Recombination in Silicon. Energy Procedia 2012;27:88–94, doi:10.1016/j.egypro.2012.07.034.
[14] Trupke T, Green MA, Würfel P, Altermatt PP, Wang A, Zhao J, Corkish R. Temperature dependence of the radiative recombination coefficient of intrinsic crystalline silicon. J. Appl. Phys. 2003;94:4930, doi:10.1063/1.1610231.
[15] Geerligs LJ, Macdonald D. Dynamics of light-induced FeB pair dissociation in crystalline silicon. Appl. Phys. Lett. 2004;85:5227, doi:10.1063/1.1823587.
[16] Schubert MC, Habenicht H, Warta W. Imaging of Metastable Defects in Silicon. IEEE J. Photovoltaics 2011;1:168–73, doi:10.1109/JPHOTOV.2011.2169942.
[17] Shockley W, Read WT. Statistics of the Recombinations of Holes and Electrons. Phys. Rev. 1952;87:835–42, doi:10.1103/PhysRev.87.835.
[18] Murphy JD, Bothe K, Krain R, Voronkov VV, Falster RJ. Parameterisation of injection-dependent lifetime measurements in semiconductors in terms of Shockley-Read-Hall statistics: An application to oxide precipitates in silicon. J. Appl. Phys. 2012;111:113709, doi:10.1063/1.4725475.
[19] Martini R, Sivaramakrishnan RH, Depauw V, van Nieuwenhuysen K, Gordon I, Gonzalez M, Poortmans J. Improvement of seed layer smoothness for epitaxial growth on porous silicon. MRS Proc. 2013;1536:97–102, doi:10.1557/opl.2013.748.